

STATOR WINDING INTER-TURN SHORT-CIRCUIT MODELLING OF A SQUIRREL-CAGE INDUCTION MOTOR*

ANDRZEJ RADECKI

Łódź University of Technology, Institute of Automatics,
ul. Stefanowskiego 18/22, 90-924 Łódź, Poland, e-mail: andrzej.radecki@p.lodz.pl

Abstract: A mathematical model of a squirrel-cage induction motor with inter-turn short-circuits in stator phases is presented in this paper. In the proposed mathematical model an extent and angular localization of short-circuit faults are determined using a simple form of short-circuit coefficient matrices. The model does not require any additional motor parameters than those that are required for conventional model of healthy induction motor. Comparative results obtained through computer simulations and from a laboratory test-stand with 2.2 kW induction motor are contained in the article. The results obtained validate the proposed extended mathematical model of a squirrel-cage induction motor with inter-turn short-circuit of stator windings.

Keywords: *Squirrel-cage induction motor modelling, induction motor faults, stator winding inter-turn short-circuit.*

1. INTRODUCTION

Induction motor (IM) drives are used widely in the industry. Their advantages compared to other types of electric motors are mainly high reliability and durability. Reliability of drive systems with an IM can be increased by using diagnostic algorithms implemented on-line or Fault-Tolerant Control (FTC) strategies [1]–[5].

Faults of an IM are related to the mechanical damage of rotor bearings, electrical damage of the stator windings and the rotor cage bars [6]. According to IEEE and EPRI (Electric Power Research Institute) the share of common faults is between: 40%–42% for bearing faults, 28%–38% for electrical stator faults, and 8%–10% for electrical faults of a rotor [5]. The most important electrical faults of an IM are related to: full or partial inter-turn short-circuit of stator winding fault, open stator phase fault and stator asymmetry fault due to increased stator phase resistance. In the areas of an IM diagnostics and FTC algorithms an important role is played by mathematical models that reflect the additional equations describing the IM faults. Those models offer

* Manuscript received March 30, 2016; revised May 30, 2016.

the possibility of performing non-invasive research on precise diagnostic methods and control algorithms through simulation environments. Mathematical models of an IM can be classified according to the type of damage being modelled. There are models that consider broken bars of the rotor cage, eccentric position of the rotor or electrical damage of the stator [7]–[14]. The main electrical fault of the stator is an adjacent turn short-circuit caused by insulation damage. Therefore mathematical models, which describe this fault, are especially important.

Mathematical models of an IM, which consider the stator winding short-circuits, are the subject of many research works [7]–[14]. Parameters of IM models or synchronous motors, with stator winding short-circuits, are calculated using extended methods compared to the fully symmetrical IM [12]–[14] or the finite element methods [15]. Some methods of IM estimation of model parameters require an exact knowledge of stator winding topology [14]. This knowledge allows the electric machine inductances to be precisely calculated. Mathematical models presented by the authors of publications mainly concern short-circuit occurring in a single phase of stator. In this paper, a simplified mathematical model of squirrel-cage IM is presented, which considers short-circuit occurring in any phase of stator (Fig. 1), in which the extent and the angular position of a short-circuit, is determined using coefficient matrices.

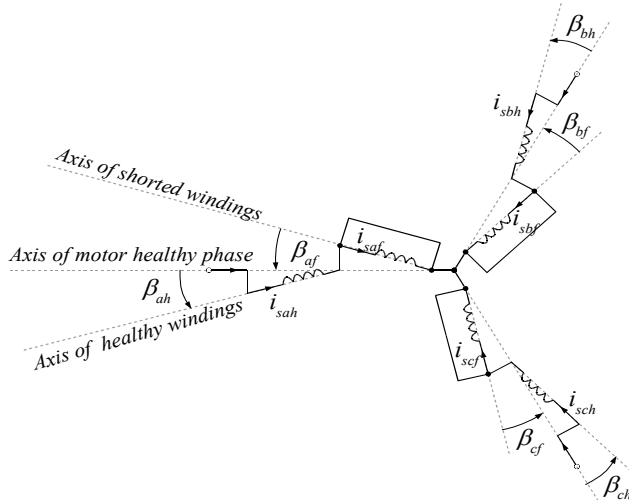


Fig. 1. The model of induction motor stator windings that considers phase inter-turn short-circuits with angular offset between healthy and faulty parts of coils

The angular offset introduced between healthy and faulty parts of stator windings gives the possibility to model a randomly placed occurrence of short-circuit that can lead to unbalanced windings. Self-inductances and mutual-inductances of an IM are estimated in a way that does not require additional knowledge about their topology

and are sufficient for correct determination of current waveforms in both healthy and faulty parts of phase windings.

An exact knowledge about stator winding currents is essential for high quality IM diagnostic methods and FTC strategies. The mathematical model of an IM proposed is described in natural coordinate system. This enables a simple modelling of stator winding asymmetry and leads to proper IM model parameters calculation of healthy and faulty stator winding currents. A validation of the proposed mathematical model of an IM is shown in this article in comparison to the results achieved from real test-stand with the motor SIEMENS 1LA7096-2AA10-Z with a rated power of 2.2 kW.

2. THE MATHEMATICAL MODEL OF THE INDUCTION MOTOR

A typical mathematical model of the squirrel-cage induction motor, expressed in a natural coordinate system, can be described as follows

$$\mathbf{U}_s = \mathbf{R}_s \mathbf{I}_s + \frac{d\boldsymbol{\Psi}_s}{dt}, \quad \mathbf{0} = \mathbf{R}_r \mathbf{I}_r + \frac{d\boldsymbol{\Psi}_r}{dt}, \quad \boldsymbol{\Psi}_s = \mathbf{L}_{ss} \mathbf{I}_s + \mathbf{L}_{sr} \mathbf{I}_r, \quad \boldsymbol{\Psi}_r = \mathbf{L}_{rs} \mathbf{I}_s + \mathbf{L}_{rr} \mathbf{I}_r, \quad (1)$$

where: \mathbf{U}_s , \mathbf{I}_s – vectors of phase voltages and currents of the stator, \mathbf{I}_r – vector of rotor phase currents, $\boldsymbol{\Psi}_s$, $\boldsymbol{\Psi}_r$ – vectors of stator and rotor fluxes, and

$$\begin{aligned} \mathbf{R}_s &= \begin{bmatrix} R_{sa} & 0 & 0 \\ 0 & R_{sb} & 0 \\ 0 & 0 & R_{sc} \end{bmatrix}, \quad \mathbf{R}_r = \begin{bmatrix} R_{ra} & 0 & 0 \\ 0 & R_{rb} & 0 \\ 0 & 0 & R_{rc} \end{bmatrix}, \quad \mathbf{L}_{ss} = \begin{bmatrix} L_{sasa} & L_{sasb} & L_{sasc} \\ L_{sbsa} & L_{sbsb} & L_{sbsc} \\ L_{scsa} & L_{scsb} & L_{scsc} \end{bmatrix}, \\ \mathbf{L}_{rr} &= \begin{bmatrix} L_{rara} & L_{rarb} & L_{rarc} \\ L_{rbra} & L_{rbrb} & L_{rbrc} \\ L_{rcra} & L_{rcrb} & L_{rcrc} \end{bmatrix}, \quad \mathbf{L}_{sr} = \begin{bmatrix} L_{sara} & L_{sarb} & L_{sarc} \\ L_{sbra} & L_{sbrb} & L_{sbrc} \\ L_{scra} & L_{scrb} & L_{scrc} \end{bmatrix}, \quad \mathbf{L}_{rs} = \mathbf{L}_{sr}^T, \end{aligned} \quad (2)$$

where: indexes a, b, c are phases, and indexes s and r denote stator and rotor.

Electromagnetic torque, which an IM generates, can be calculated using

$$M_{el} = \mathbf{I}_s^T \frac{d\mathbf{L}_{sr}}{d\Theta} \mathbf{I}_r \cdot p, \quad (3)$$

where: Θ – position of the rotor electric angle, p – number of pole pairs.

It can be assumed that healthy IM is fully symmetrical. In this case, parameter matrices from equations (2) can be reduced to the following form

$$\begin{aligned} \mathbf{R}_s &= R_s \cdot \mathbf{I}, \quad \mathbf{R}_r = R_r \cdot \mathbf{I}, \quad \mathbf{L}_{ss} = L_{\delta s} \cdot \mathbf{I} + L_{ms} \cdot \cos(\alpha), \\ \mathbf{L}_{rr} &= L_{\delta r} \cdot \mathbf{I} + L_{mr} \cdot \cos(\alpha), \quad \mathbf{L}_{sr} = L_{sr} \cdot \cos(\alpha + \Theta), \quad \mathbf{L}_{rs} = \mathbf{L}_{sr}^T, \end{aligned} \quad (4)$$

where: R_s , R_r – resistances of stator and rotor phases, $L_{\delta s}$, $L_{\delta r}$ – leakage inductances of stator and rotor phases, L_{ms} , L_{mr} – main inductances of the stator and the rotor, L_{sr} – mutual inductance between the stator and the rotor, \mathbf{I} – the identity matrix of size 3×3 , and both the operation \cos and its argument are defined as follows

$$\cos(A_{n \times n}) = \begin{bmatrix} \cos(A_{11}) & \dots & \cos(A_{1n}) \\ \vdots & \ddots & \vdots \\ \cos(A_{n1}) & \dots & \cos(A_{nn}) \end{bmatrix}, \quad \alpha = \begin{bmatrix} 0 & \frac{2\pi}{3} & -\frac{2\pi}{3} \\ -\frac{2\pi}{3} & 0 & \frac{2\pi}{3} \\ \frac{2\pi}{3} & -\frac{2\pi}{3} & 0 \end{bmatrix}. \quad (5)$$

3. STATOR WINDING INTER-TURN SHORT-CIRCUIT MODELLING OF A SQUIRREL-CAGE INDUCTION MOTOR

Taking into account stator winding inter-turn short-circuit, equations (1) have to be extended to the model of an IM considering faulty state. Shorted parts of coil can be treated as an extra set of stator windings with zero-voltage vector on their terminals. In [8], [12], [13], equations (1) were extended to meet this assumption, which leads to the following form

$$\begin{aligned} \mathbf{U}_s &= \mathbf{R}_{sh}\mathbf{I}_{sh} + \frac{d\boldsymbol{\Psi}_{sh}}{dt}, \quad \mathbf{0} = \mathbf{R}_{sf}\mathbf{I}_{sf} + \frac{d\boldsymbol{\Psi}_{sf}}{dt}, \\ \mathbf{0} &= \mathbf{R}_r\mathbf{I}_r + \frac{d\boldsymbol{\Psi}_r}{dt}, \quad \boldsymbol{\Psi}_r = \mathbf{L}_{rsh}\mathbf{I}_{sh} + \mathbf{L}_{rsf}\mathbf{I}_{sf} + \mathbf{L}_{rr}\mathbf{I}_r, \\ \boldsymbol{\Psi}_{sh} &= \mathbf{L}_{shsh}\mathbf{I}_{sh} + \mathbf{L}_{shsf}\mathbf{I}_{sf} + \mathbf{L}_{shr}\mathbf{I}_r, \quad \boldsymbol{\Psi}_{sf} = \mathbf{L}_{sfsh}\mathbf{I}_{sh} + \mathbf{L}_{sfsf}\mathbf{I}_{sf} + \mathbf{L}_{sfr}\mathbf{I}_r, \end{aligned} \quad (6)$$

where” \mathbf{I}_{sh} , \mathbf{I}_{sf} – vectors of phase currents in healthy and faulty parts of windings, $\boldsymbol{\Psi}_{sh}$, $\boldsymbol{\Psi}_{sf}$ – vectors of fluxes related to healthy and faulty parts of windings, and

$$\mathbf{R}_{sh} = \begin{bmatrix} R_{sah} & 0 & 0 \\ 0 & R_{sbh} & 0 \\ 0 & 0 & R_{sch} \end{bmatrix}, \quad \mathbf{R}_{sf} = \begin{bmatrix} R_{saf} & 0 & 0 \\ 0 & R_{sbf} & 0 \\ 0 & 0 & R_{scf} \end{bmatrix}, \quad \mathbf{L}_{sxr} = \begin{bmatrix} L_{saxra} & L_{saxrb} & L_{saxrc} \\ L_{sbxra} & L_{sbxrb} & L_{sbxrc} \\ L_{scxra} & L_{scxrb} & L_{scxrc} \end{bmatrix}, \quad (7a)$$

$$\mathbf{L}_{sxsy} = \begin{bmatrix} L_{saxsay} & L_{saxsby} & L_{saxscy} \\ L_{sbxsay} & L_{sbxsby} & L_{sbxscy} \\ L_{scxsay} & L_{scxsby} & L_{scxscy} \end{bmatrix}, \quad \mathbf{L}_{rsx} = \mathbf{L}_{sxr}^T, \quad \mathbf{L}_{sysx} = \mathbf{L}_{sxsy}^T, \quad (7b)$$

where indexes h and f denote healthy and faulty parts of the phase windings, respectively, and each of the indexes x and y represents either h or f index.

An electromagnetic torque generated by the motor can be obtained from

$$M_{el} = \begin{bmatrix} \mathbf{I}_{sh} \\ \mathbf{I}_{sf} \end{bmatrix}^T d \begin{bmatrix} \mathbf{L}_{shr} \\ \mathbf{L}_{sfr} \end{bmatrix} \mathbf{I}_r = \mathbf{I}_{sh}^T \frac{d\mathbf{L}_{shr}}{d\Theta} \mathbf{I}_r + \mathbf{I}_{sf}^T \frac{d\mathbf{L}_{sfr}}{d\Theta} \mathbf{I}_r . \quad (8)$$

4. THE SIMPLIFIED FORM OF THE IM MODEL PARAMETER MATRICES

Computation of matrices (7), which describe self and mutual inductances, is a complicated task. In the general case, calculation of coil inductances in complex magnetic systems is made on the basis of functions describing the distribution of a coil inductance [12]–[14] or using finite element methods [15].

To simplify the problem of determining inductance matrices, which are a part of equations (6), the following assumptions were made:

1. Healthy and faulty windings are considered as concentrated.
2. Healthy and faulty windings are free of magnetic saturation.
3. In a short-circuit of winding k_{xf} part (where k_{xf} denotes short-circuit extent in phase x and is in the range of $<0,1>$), a k_{xh} part (where $k_{xh} = 1 - k_{xf}$) remains healthy. The number of faulty and healthy winding turns can be described as follows

$$n_{sx} = n_{sx} \cdot k_{xf}, \quad n_{sxh} = n_{sx} \cdot k_{xh} . \quad (9)$$

4. An axis of faulty windings can have angular offset β_{xf} with respect to the axis of healthy IM phase windings. Because weighted sum of angular position of healthy and faulty windings (which takes into account the number of shorted winding turns) should be the same as for IM in healthy state, an angular position of both winding parts can be calculated from the relationship

$$\beta_{xf} \cdot k_{xf} + \beta_{xh} \cdot k_{xh} = 0 \Rightarrow \beta_{xh} = \frac{-k_{xf}}{k_{xh}} \cdot \beta_{xf} . \quad (10)$$

The foregoing considerations lead to generalized form of a mathematical model of an IM with matrices of parameters that comply with the requirements for assumptions on extent and angular offset of winding faults

$$\begin{aligned}
\mathbf{R}_{sh} &= \mathbf{R}_s \circ \mathbf{k}_h, \quad \mathbf{R}_{sf} = \mathbf{R}_s \circ \mathbf{k}_f, \\
\mathbf{L}_{shsh} &= (\mathbf{L}_{\delta s} \cdot \mathbf{I} + \mathbf{L}_{ms} \cdot \cos(\alpha - (\boldsymbol{\beta}_h - \boldsymbol{\beta}_h^T))) \circ \mathbf{k}_h \circ \mathbf{k}_h^T, \\
\mathbf{L}_{sfsf} &= (\mathbf{L}_{\delta s} \cdot \mathbf{I} + \mathbf{L}_{ms} \cdot \cos(\alpha - (\boldsymbol{\beta}_f - \boldsymbol{\beta}_f^T))) \circ \mathbf{k}_f \circ \mathbf{k}_f^T, \\
\mathbf{L}_{shsf} &= \mathbf{L}_{ms} \cdot \cos(\alpha - (\boldsymbol{\beta}_h - \boldsymbol{\beta}_f^T)) \circ \mathbf{k}_h \circ \mathbf{k}_f^T, \quad \mathbf{L}_{sfsh} = \mathbf{L}_{shsf}^T, \\
\mathbf{L}_{shr} &= \mathbf{L}_{sr} \cdot \cos(\alpha + \boldsymbol{\Theta} - \boldsymbol{\beta}_h) \circ \mathbf{k}_h, \quad \mathbf{L}_{rsh} = \mathbf{L}_{shr}^T, \\
\mathbf{L}_{sfr} &= \mathbf{L}_{sr} \cdot \cos(\alpha + \boldsymbol{\Theta} - \boldsymbol{\beta}_f) \circ \mathbf{k}_f, \quad \mathbf{L}_{rsf} = \mathbf{L}_{sfr}^T,
\end{aligned} \tag{11}$$

where the operator \circ is the entry-wise product, and short-circuit matrices \mathbf{k}_h and \mathbf{k}_f as well as winding angular offset matrices $\boldsymbol{\beta}_h$ and $\boldsymbol{\beta}_f$ are defined as follows:

$$\begin{aligned}
\mathbf{k} &= \begin{bmatrix} k_a \\ k_b \\ k_c \end{bmatrix}, \quad \mathbf{k}_f = \mathbf{k}[111], \quad \mathbf{k}_h = 1 - \mathbf{k}_f, \quad \boldsymbol{\beta} = \begin{bmatrix} \beta_a \\ \beta_b \\ \beta_c \end{bmatrix}, \\
\boldsymbol{\beta}_f &= \boldsymbol{\beta}[111], \quad \boldsymbol{\beta}_h = -\boldsymbol{\beta}_f \circ \mathbf{k}_f ./ \mathbf{k}_h,
\end{aligned} \tag{12}$$

where coefficients $k_a, k_b, k_c \in \langle 0, 1 \rangle$, denote extent of short-circuit in faulty windings of phase a, b and c of the stator, and $\beta_a, \beta_b, \beta_c$ their angular offset. The operator $./$ is the right-side entry-wise division.

5. THE RESULTS OF SIMULATION AND LABORATORY TESTS

To verify the proposed mathematical model of the induction motor, taking into account inter-turn short-circuit stator windings, equations (6), (8) and (11) have been implemented in the SciLab computing environment. The results of the computer simulations have been compared to the results obtained from the laboratory tests carried out using the squirrel-cage induction motor SIEMENS 1LA7096 2AA10-Z. In this machine, selected turns were cut off and led outside the stator to allow short-circuit modelling (among others, faults). During the research test, 20% of the phase winding turns was shorted. Rated parameters of IM used: $P_n = 2.20$ kW, $U_s = 400$ V, $I_s = 4.7$ A, $\cos\varphi = 0.85$, $T_n = 7.30$ Nm, $n_n = 2880$ rpm, $R_s = 3.06$ Ω , $R_r = 2.0$ Ω , $L_s = L_r = 339$ mH, $L_m = 338$ mH. Dynamic load of the motor in the laboratory tests was a flywheel mass with the moment of inertia $J = 0.14$ kgm², exceeding 30 times the moment of inertia of the machine rotor. In Figs. 2–4, waveforms of the electromagnetic torques and the selected currents are shown. The tests were designed to perform a single duty cycle of the drive with both accelerating and braking stages (Fig. 3). The simulation model of the drive system described by equations (6), (8) and (11) had the input voltage vector corresponding to the real IM on test-stand. The motor was

powered by a voltage inverter using the DTC control strategy. For better readability of the input voltage vector used in simulations, a Short Time Fourier Transform (STFT) of its single phase is shown in Fig 5c. Symbols used in the figures: i_{pom} – measured current, i_{mdl} – current acquired from computer simulation, T_{est} – electromagnetic torque estimated using shaft speed and known moment of inertia, T_{mdl} – electromagnetic torque acquired from computer simulation, T_{ref} – electromagnetic torque reference.

The waveforms of phase currents recorded on a laboratory stand with the use of oscilloscope and computed by the mathematical model described by equations (6) indicate compliance of presented model with real test-stand (Figs. 2–4).

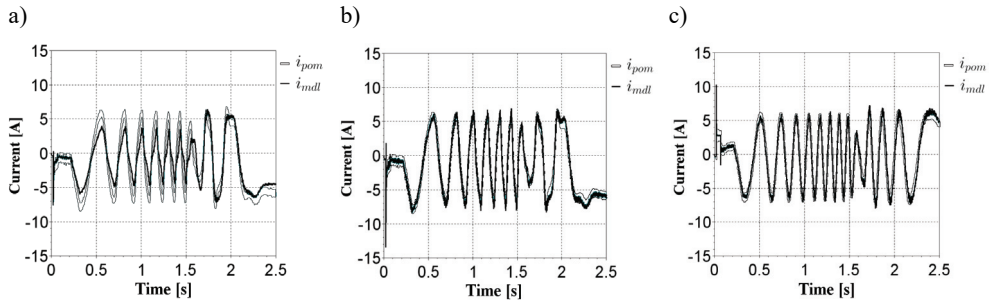


Fig. 2. Waveforms of stator phase currents for (a) 20% shorted windings and using mathematical model disregarding inter-turn short-circuits ($k_a = 0$), (b) 20% shorted windings and considering inter-turn short-circuits ($k_a = 0.2$), (c) healthy induction machine and using the mathematical model introduced

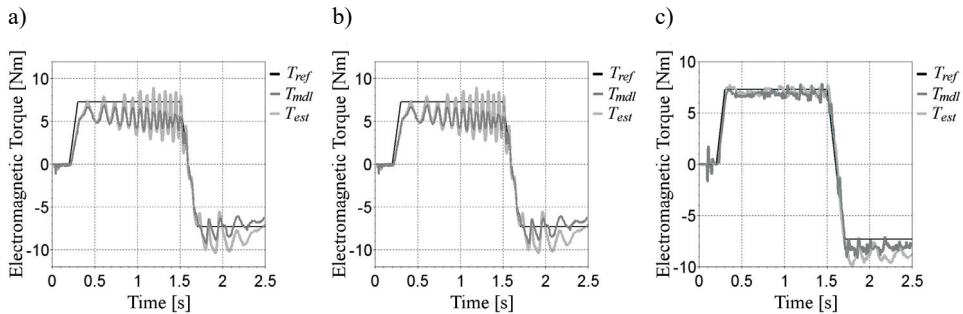


Fig. 3. Electromagnetic torques for (a) 20% shorted windings and using mathematical model disregarding inter-turn short-circuits ($k_a = 0$), (b) 20% shorted windings and considering inter-turn short-circuits ($k_a = 0.2$), (c) healthy induction machine and using the mathematical model introduced

The mathematical model described by equations (1) produces strongly deformed phase current, inconsistent with the measurements (Fig. 2a). The general machine performance acquired during the tests is shown in Fig. 3. It can be noticed that the

electromagnetic torque calculated through the IM model is exactly the same for faulty cases (Fig. 2a, 2b) regardless of the model used. Mathematical model of the induction motor with additional part of equations (that consider angular offset between healthy and faulty windings) allows for better fit of the current waveform phase shift. In the case under research test of 20% short-circuited turns, the best match of the phase shift is at $\beta_a = -0.06 \text{ rad}$. To highlight this phase alignment, the chosen time range of waveforms is presented in Fig. 4. It should be mentioned that in the faulty state of the IM, the value of angular offset was variable and depended on short-circuit location.

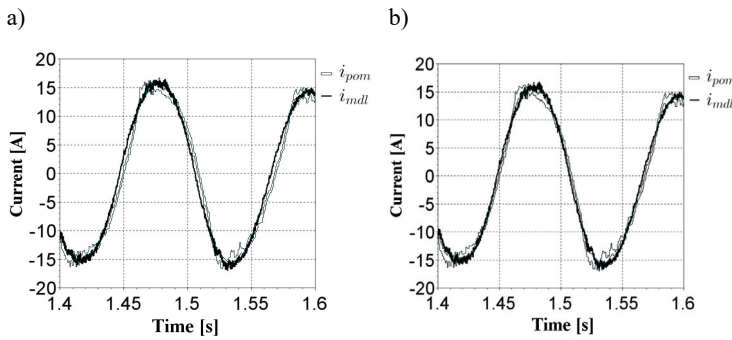


Fig. 4. Zoomed time range of shorted winding current waveforms for case of
a) disregarding angular displacement ($\beta_a = 0 \text{ rad}$), b) considering angular displacement ($\beta_a = -0.06 \text{ rad}$)

Moreover, in a healthy IM there was no phase shift between measured and calculated stator currents. Because the angular offset introduced is related to the IM construction, it is independent of the state of the machine. The influence of the shorted turns current phase shift on healthy windings current can be very useful in diagnostics and FTC strategies. This issue, however, requires further research.

For more precise analysis of current waveforms their differential spectra, calculated using STFT are shown in Figs. 5 and 6. STFT of faulty winding current estimation error is presented in Fig 5. In the whole range of analysing time, the error does not exceed 250 mA of the first harmonic for the model that considers inter-turn short-circuit. Spectra of $Q(t, f)$ coefficients, which denote estimation accuracy of calculated faulty winding current phase shift, are shown in Fig. 6. Function $Q(t, f)$ is defined as follows

$$Q(t, f) = \frac{1}{\left(|X(t, f) - Y(t, f)| + \frac{1}{q} \right) \cdot q}, \quad (13)$$

where: $X(t, f)$ – phase shift spectra of measured current, $Y(t, f)$ – phase shift spectra of calculated current, q – sensitivity coefficient ($q = 10^6/\text{rad}$).

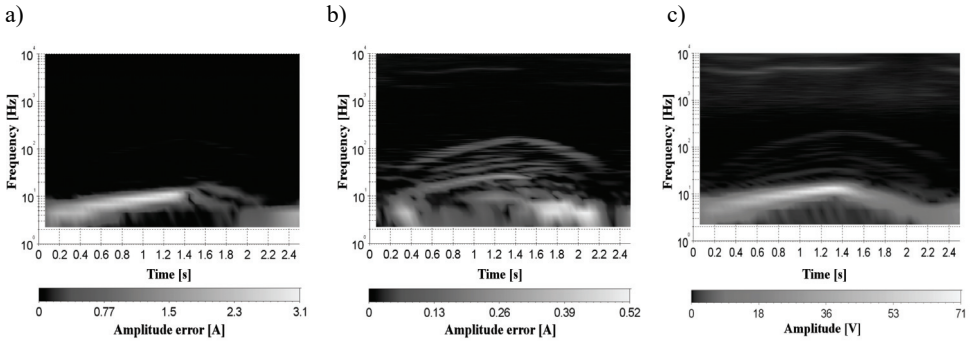


Fig. 5. Amplitude STFT spectra of (a) the difference of phase current (measured and determined by simulation) in the case of 20% shorted windings and disregarding inter-turn short-circuit in the model, (b) the difference of phase current in the case of 20% shorted windings and considering inter-turn short-circuit in the model, (c) single phase voltage used as an input for all simulations

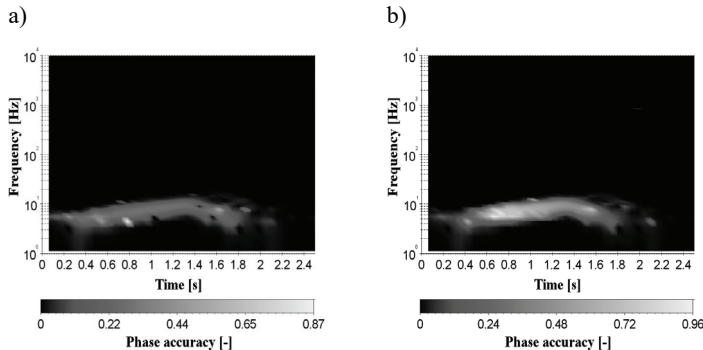


Fig. 6. Phase-shift quality index of faulty winding current first harmonic estimation in the case of (a) disregarding angular displacement ($\beta_a = 0$ rad), (b) considering angular displacement ($\beta_a = -0.06$ rad)

Considering angular offset of $\beta_a = -0.06$ rad, the quality of phase-shift of faulty windings current first harmonic estimation is much higher (Fig. 6b).

5. CONCLUSIONS

The extended mathematical model of squirrel-cage induction motor is presented in the paper. The model proposed takes into account an angular offset between faulty and healthy parts of stator windings. There is no need to know any additional induction motor IM parameters than those that are required for conventional model of healthy machine. The obtained results, included in the article, confirm that the proposed extended mathematical model allow the phase-shift of the faulty winding current to be

estimated precisely. Such an estimation of faulty windings current can be further used in high efficient FTC strategies or for precise diagnostic purposes.

REFERENCES

- [1] ZHANG Y., JIANG J., *Bibliographical review on reconfigurable fault-tolerant control systems*, Annual Reviews in Control, 2008, No. 32, 229–252.
- [2] CAMPOS-DELGADO D.U., ESPINOZA-TREJO D.R., PALACIOS E., *Fault-tolerant control in variable speed drives:a survey*, IET Electric Power Applications, 2008, No. 2, 121–134.
- [3] WIERZBICKI R., KOWALSKI C., *Stator and Rotor Faults Detection in Direct Field Oriented Closed Loop Induction Motor Drive*, Przegląd Elektrotechniczny, 2012, No. 4B, 265–269, (in Polish).
- [4] WOLKIEWICZ M., TARCHALA G., KOWALSKI C.T., *Stator windings condition diagnosis of voltage inverter-fed induction motor in open and closed-loop control structures*, Archives of Electrical Engineering, 2015, No. 1, Vol. 64, 67–79.
- [5] KHALAF S.G., HAIDER M., *Diagnosis and Fault Tolerant Control of the Induction Motors Techniques a Review*, Australian Journal of Basic and Applied Sciences, 2010, 227–246.
- [6] KOWALSKI CZ. T., *Monitoring and diagnostics of the induction motor faults using neural networks*, Scientific Papers of the Institute of Electrical Machines, Drives and Measurements of the Wrocław University of Technology, ser. Monographs, 2005, Vol. 57, No. 18, (in Polish).
- [7] ANTAL M., ANTAL L., ZAWILAK J., *Testing of failures in stator winding of squirrel-cage induction motor*, Electrical Machines – Transaction Journal, 2007, No. 76, 83–88, (in Polish).
- [8] WIECZOREK M., ROSOŁOWSKI E., *Simulation analysis of induction motor turn-to-turn faults in stator windings*, Scientific Papers of the Institute of Electrical Power Engineering of the Wrocław University of Technology, Present Problems of Power System Control, 2011, No. 1, 43–53.
- [9] KOWALSKI C., WOLKIEWICZ M., WIERZBICKI R., *Converter-fed induction motor modelling with inter-turn stator faults*, Przegląd Elektrotechniczny, 2010, No. 4, 220–224, (in Polish).
- [10] GHATE V.N., DUDUL S.V., DHOLE G. M., *Generalized Model of Three-Phase Induction Motor for Fault Analysis*, IEEE Int. Conf. Computational Technologies in Electrical and Electronics Engineering, 2008, 232–237.
- [11] LIANG B., BALL A.D., IWNICKI S.D., *Simulation and fault detection of three-phase induction motors*, IEEE Conference on Computers, Communications, Control and Power Engineering, 2008, Vol. 3, 1813–1817.
- [12] RAZAFIMAHEFA T.D., HERAUD N., SAMBATRA E.J.R., WAILLY O., *Comparative study of inter-turn short circuit fault in stator and rotor windings on a small and medium power wound rotor induction machine*, Conference on Control and Automation, 2015, 184–189.
- [13] SAHRAOUI M., GHOGGAL A., ZOIZOU S.E., ABOUBOU A., RAZIK H., *Modelling and Detection of Inter-Turn Short Circuits in Stator Windings of Induction Motor*, 32nd Annual Conference on IEEE Industrial Electronics, 2006, 4981–4986.
- [14] MAOUCHE Y., BOUSSAID A., BOUCHERMA M., KHEZZAR A., *Modeling and Simulation of Stator Turn Faults. Detection Based on Stator Circular Current and Neutral Voltage*, 9th IEEE Int. Symp. on Diagnostics for Electric Machines, 2013, 263–268.
- [15] VASEGHI B., TAKORABET N., NAHID-MOBARAKEH B., MEIBODY-TABAR F., *Modelling and study of PM machines with inter-turn fault dynamic model–FEM model*, Electric Power Systems Research, 2011, No. 81, 1715–1722.